DISTORTIONAL BUCKLING OF NONPRISMATIC MONOSYMMETRIC BRACED CANTILEVERS

A Thesis Submitted
in Partial Fulfilment of the Requirements
for the Degree of

MASTER OF TECHNOLOGY

by

BHISE PRASHANT C.

to the

DEPARTMENT OF CIVIL ENGINEERING
INDIAN INSTITUTE OF TECHNOLOGY, KANPUR

FEBRUARY, 1994

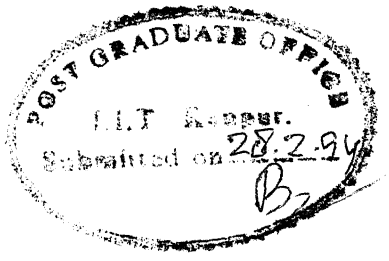

CERTIFICATE

It is certified that the work contained in the thesis entitled DISTORTIONAL BUCKLING OF NONPRISMATIC MONOSYMMETRIC BRACED CANTILEVERS by Bhise Prashant C. has been carried out under my supervision and that this work has not been submitted elsewhere for a degree.

(Ashwini Kumar)

Professor
Department of Civil Engineering
Indian Institute of Technology
Kanpur

Feb, 1994

ABSTRACT

This investigation deals with distortional buckling of non-prismatic cantilever beams. A finite element formulation is developed and its convergence and accuracy are demonstrated. Elastic buckling solutions are obtained for a mono-symmetric cantilever beam under a concentrated load at its end. The effect of both the flange and the web tapering along with the effect of the application of load at top flange/ shear centre on the buckling load are studied. The influence of different types of braces and their location is examined in detail on distortional buckling of beam for various degrees of mono-symmetry.

Dedicated to ....

my beloved

family members

ACKNOWLEDGEMENT

I would like to express my sincere gratitude and profound appreciation to Dr. Ashwini Kumar, my thesis supervisor for being constant source of strength and inspiration during the entire course of this work. I am extremely thankful to him for giving me the complete work freedom, thus helping me to gain confidence to work independently. I am highly indebted to him for all those fruitful discussions and expert advice throughout the research work.

Sincere, thanks are due to the faculty of this Institute for being constant source of knowledge and inspiration.

Special thanks to Mr. Umesh Dindore ,Mr. Samarth Agarwal and Mr. Nagpure for their timely help and valuable suggestions. Further, I wish to express my special thanks to Ashfaq, Gaurav and Nagpure for allowing me to use their computer facility.

Finally, I am very much grateful to my numerous friends who have made my stay over here, the most cherish memory for the rest of my life.

Prashant C. Bhise

CONTENTS

List Of Figures

List Of Symbols

A_{ft}, A_{fb} = area of the top and the bottom flanges respectively.

b_t , b_b = width of the top and the bottom flange respectively.

$[B_w]$ = element dimension matrix for web strains.

$[C_w]$, $[C]$ = coefficient matrix associated with displacement functions for web and total cross-section respectively.

D_f = plate rigidity of flanges = $E T^3 / [12 (1 - \upsilon^2)]$.

$[D_w]$ = web property matrix.

E = Young's modulus of elasticity.

f = cubic function of z in web displacement curve.

G = shear modulus of steel.

$[G]$ = global stability matrix.

$[g]$ = element stability matrix.

H = h / L

h = distance between flanges centroid.

I_x = moment of inertia of whole section about x-axis.

I_y = moment of inertia of whole section about y-axis.

I_{yft}, I_{yfb} = moment of inetia of the top and the bottom flange, resectively, about y-axix

J = torsion constant.

$[K]$ = global stiffness matrix.

$[k]$ = element stiffness matrix.

$\bar{k}$ = beam parameter defined in eq. (2.3).

L = length of the element.

l = length of the beam.

$[M]$ = displacement function matrix for the flange.

$[N_w]$, $[N]$ = displacement function matrix for the web.

M_1 , M_2 = end moment on the element.

M_x = moment at any section x along the beam.

$\{ Q \}$ = vector of global degrees of freedom.

$\{ q \}$ = vector of element degrees of freedom.

T = thickness of the governing flange.

t = the web thickness.

U = total strain energy stored in the beam.

U_{fu}, $U_{f\phi}$, U_w = the flange in-plane bending, out-of-plane bending and twisting and the web strain energy.

u_t u_b u_w = lateral displacement of the top flange, the bottom flange and the web, respectively.

$\{ u \}$ = vector of flange displacements in eq (2.4).

V = total work-done during buckling by the beam element.

V_1 ,V_2 = end shear forces on the beam element.

V_d = work done by concentrated load not at shear centre.

V_{fu} , $V_{f\phi}$ = work-done associated with the in-plane flange deformation and the out of flange deformations.

V_t ,V_b = top and bottom flange vertical displacement.

V_w = web vertical displacement.

W_{od} = distortional buckling load.

W_{or} = lateral-torsional buckling load.

Y = 2 y / h

Z = z / l

x, y, z = cartesian axes.

λ = buckling load factor.

Π = total potential

υ = Poisson's ratio.

$\alpha_1, \alpha_2, \ldots, \alpha_{12}$ = polynomial coefficients for flange displacements.

$\{ \alpha \}$ = vector of flange displacement coefficients.

$\{ \alpha_w \}$ = vector of web displacement coefficients.

$\{ \delta \}$ = vector of element nodal displacements.

σ_t , σ_b = longitudinal stresses in the top and the bottom flanges.

σ = longitudinal stress in the web.

ρ = mono-symmetry parameter given in eq. (2.1)

τ = shear stress in the web.

ϕ_t , ϕ_b = rotation of the top and the bottom flanges respectively.

D^n = differential operator of order n

CHAPTER I

INTRODUCTION

1.1 Stability

The stability of structure essentially means the stability of its equilibrium configuration or state. In mathematical sense, stability is usually interpreted to mean that the infinitesimal disturbance will cause only infinitesimal departure from the given equilibrium position. In practical sense, an equilibrium state of a structure or a system is said to be stable if accidental forces, shocks, vibrations, eccentricities, imperfections or other possible irregularities do not cause the system to depart excessively from its designed position.

In designing structures, care should be taken that the stresses developed do not exceed certain limits, which may otherwise lead to failure. Two kinds of failure can be associated with the structure (i) failure with respect to material behaviour, (ii) form failure. In the first case, stresses exceed the given safe limits resulting in formations of cracks which cause failure. In the second case, the stresses do not exceed the safe values but structure may not keep up the forms in which it is designed. Also, loads on a structure could be tensile and/or compressive. The loss of stability due to tensile loads falls in the broad category of material instability, whereas the stability loss under compressive load is termed as

structural (or geometric or form) instability, commonly known as buckling.

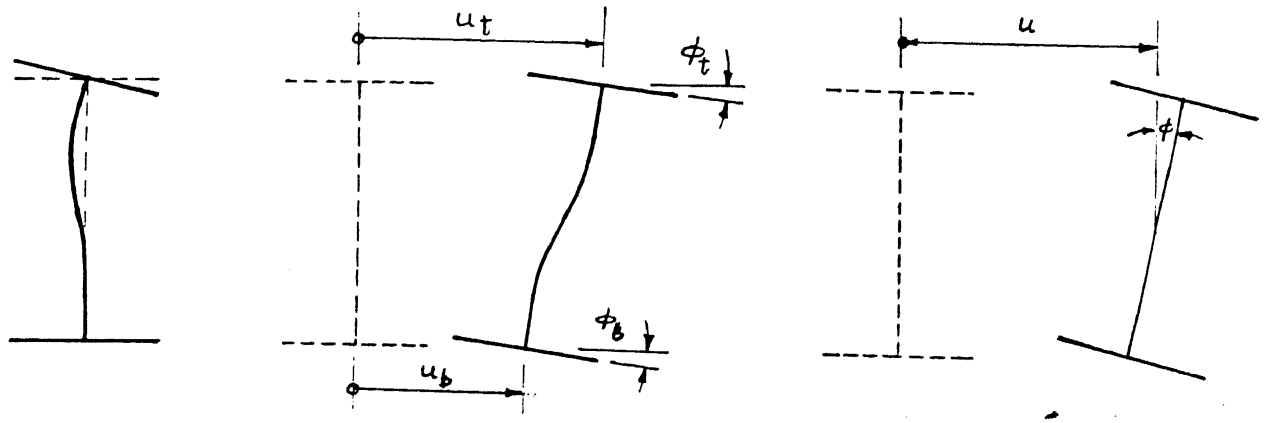

(a) Local Buckling (b) Distortional Buckling (c) Lateral-Torsional Buckling

Fig. 1.1 MEMBER BUCKLING MODES

Consider the case of an I-beam under the action of transverse load. The beam may buckle in three ways,(i) local buckling,(ii) lateral buckling, (iii) distortional buckling, as shown in Fig. 1.1. The local buckling is characterized by the change in cross-section geometry without overall lateral displacements or twist. It can be further subdivided into flange buckling , web buckling or coupled buckling (in which both the web and the flange buckle together). Lateral buckling involves lateral displacements and/or twist without local changes in the cross-section geometry. It is also possible for a member to buckle into a mode which combines lateral displacement and twist, together with local changes in the cross-section geometry. This type of buckling is as termed distortional buckling. The web distortion which allows the flanges to deflect laterally with comparatively little twist, reduces the effective torsional resistance of the member and consequently reduces the resistance to

flexure-torsional buckling. The effect has been found to be more significant in plate girders with slender, unstiffned webs. More generally, distortional buckling occurs in a mode which is intermediate between the local buckling (which occurs in very thin webs) and the lateral buckling (which occurs in members of thicker web by ignoring any distortion).

When a thin walled member of mono-symmetric I-section twists, the longitudinal normal stress due to the axial force and/ or the moment exerts torque about the axis of twist. This disturbing torque is commonly referred as the Wagner Effect, which results in an effective increase or decrease in the torsional stiffness depending on whether the axial force is tensile or compressive, and whether the smaller flange is in compression or in tension.

The elastic buckling capacity of a member may be greatly enhanced by the introduction of some forms . This could be achieved by one or more discrete braces, or by a continuous medium such as a diaphragm. A discrete brace may act to restrain either the lateral displacement or the twist or both in the beam cross-section at the brace point. It may also provide some minor-axis rotational or warping restraints. Most of the bracing arrangements [Fig. 1.2 a] in an I-beam may be represented by an idealized spring system consisting of an elastic lateral brace at a certain distance above the shear centre of cross-section and an elastic rotational brace [Fig. 1.2 b]. A full brace, as oppose to a partial brace, prevents beam from lateral translation and rotation in the cross-sectional plane at the braced point.

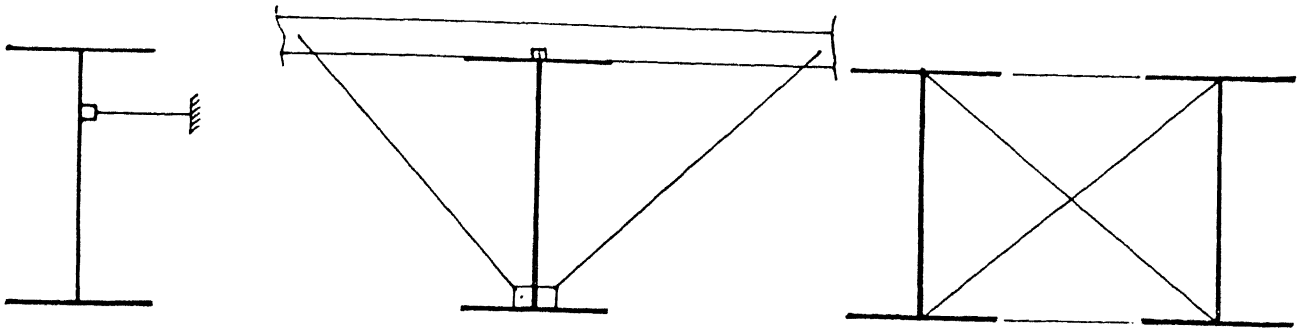

(a) Typical Braces

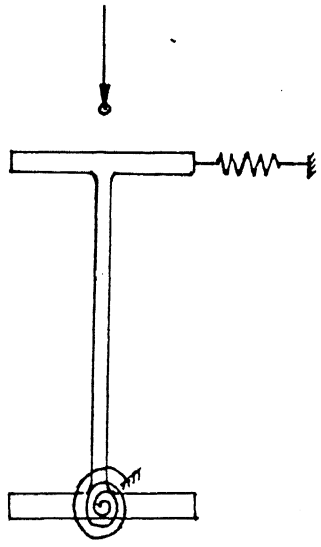

(b) Idealized Braces

Fig. 1.2 TYPES OF BRACES

1.2 Techniques For Buckling Analysis

There are a large number of techniques available which can be grouped under two general approaches viz.the static-kinematic approach and the work-energy approach. The two approaches correspond to the

different strategies used in satisfying the state of neutral equilibrium for the deformed member.

In the static-kinematic approach, the field differential equations are derived from (a) the assumed stress-strain laws, (b) equilibrium equations and (c)strain-displacement relations . The last two conditions are obtained from static and geometric considerations on a free body of the deformed member. Only in some rare cases closed form analytical solutions are possible, whereas using numerical technique such as the finite difference method, the finite integral method and the Galerkin's method one can obtain reasonably accurate results.

In the work energy approach the equilibrium condition of the deformed member is satisfied via the virtual work concept. This can be done by establishing the potential energy functional and assuming the external forces to be unchanged during displacement variation. The important principle which applies for elastic problems is the principle of energy conservation. On the basis of the principle of energy conservation and the principle of stationary potential energy, various energy methods were proposed by early researchers e.g. the Timoshenko-energy method, the Rayleigh-Ritz method and the finite element method (FEM). The FEM is an extension of the Reyleigh-Ritz method in that it involves the division of the structural member into member elements.

1.3 Literature Review

The early work on elastic buckling of I-beams remained confined to doubly-symmetric cross-sections. This led to several theoretical and experimental studies resulting in the development of approximate formulae and design charts which are now available in standard texts, e.g. Timoshenko (1961), Trahair (1988). Anderson and Trahair (1972) presented results for simply supported and cantilever mono-symmetric I-beams with concentrated and distributed loads and investigated the influence of the load height above the shear center on the elastic buckling moment. They proposed some modification factor to approximate the maximum moment in terms of the critical moment for buckling of a doubly symmetric I-beam under a moment gradient. This, and similar other studies on mono-symmetric beams, highlighted a difficulty : how best to determine the mono symmetric section property so that the flexure-torsional buckling moment could be expressed in a convenient form. This difficulty was overcome by Kitiporanchai and Trahair (1980) by introducing a new mono-symmetric parameter and thus simplifying the complicated expression being used in earlier investigations. This work led to more detailed studies of mono-symmetric beams by Wang and kitiporanchai (1986)for a simply supported beam under a uniform moment. Subsequently Wang and Kitiporanchai (1989) introduced few more additional parameters and investigated the mono-symmetric effect under various loading conditions.

For tapered mono-symmetric I-beams, Kitiporanchai and Trahair (1975) showed that the shear centre axis is not parallel to the

centroidal axis. Thus the minor axis bending moment and the torsion can not be separated. A finite element formulation for such beams was developed by Bradford (1988). He investigated the effect of flange tapering and web tapering on the elastic critical buckling loads for various degree of mono-symmetry. Kumar and Shah (1991,1993) also studied the effect of two way tapering of simply supported I-beam and beam-columns for various loading conditions and compared the results with those obtained using IS:800 specifications.

The first study on distortional buckling of cantilevers in the open literature is available due to Johnson and Will (1974). In this study two relatively fine meshes of plane-stress bending finite elements were used. Rectangular plate elements were used to model a cantilever beam loaded at its end and a simply supported beam loaded at midspan by a concentrated load applied at the top flange. These results were later verified by Hancock and Trahair (1978) using energy method. They also presented some approximate closed form solutions which could be used for design purposes. Hancock (1978) investigated the buckling of an I-beam bent about the major axis and determined the interaction between the local distortional and the flexure-torsional modes. Later Hancock and Trahair (1980) used the finite strip method to study the effect of web-distortion on elastic-flexure torsional buckling of simply supported beam-columns in uniform bending; a closed form solution was obtained as an interaction equation between the critical moment and loads. Bradford (1990) studied the effect of distortion on beams of tee-section under a uniform moment using a fine mesh of elements for discretization of beam. Bradford and Trahair (1981) developed a line finite element method for the analysis of distortional

buckling of doubly symmetric I-beams. This method used line elements for beam discretization but allowed the cross-section to distort. Later, this formulation was modified by Bradford (1992) to take into account the effect of the load height above shear centre.

Among the early studies on elastic buckling of beams with discrete braces, the study by Flint et al (1973) presented theoretical stiffness requirement for beams and columns with midspan lateral braces. Much later, Kitiporanchai et al (1984) investigated the effect of providing braces on the critical load of cantilever beams. But, the most notable reference is that of Wang et al (1986) on elastic lateral buckling of mono-symmetric cantilevers. In this investigation the influence of lateral, rotational and the full brace at various locations along the length of beam and of the load-height above shear centre was demonstrated on the critical buckling moment. Bradford (1988) developed the finite strip method to study the effect of web distortion on the critical load of mono-symmetric I-beams with stiffened webs. However, this method proved to be cumbersome for such applications.

1.4 Scope And Aim Of Investigation

Modern methods of fabricating steel members allow welded I-beams to be made easily, and it is often economical to produce such beams with thin unstiffned webs and unequal flanges. In such cases, the distortion of the cross-section is likely to modify the elastic buckling stress of beams. The elastic buckling stresses are important

for design since these are directly used in obtaining maximum permissible stresses.

As has been pointed out in the previous section, most of the studies concerning cantilever beams have been confined to investigating the lateral-torsional buckling of symmetric/mono-symmetric I-beams, with or without web/flange tapering. Investigations on distortional buckling are rather few and these too have been restricted to symmetric I-sections. Except the work of Bradford (1980) no study appears to be available on the distortional buckling of mono-symmetric sections.

While designing a cantilever beam it could be economical to design it by taking into consideration the tapering of its web and/or flange. Moreover, the buckling capacity may get enhanced by the introduction of some form of intermediate braces. Hence, this investigation aims at studying the distortional buckling of mono-symmetric, braced, cantilever beams with web and flange tapering. It makes an attempts to

* study the effect of the mono-symmetry on the buckling load of different cross-sections for various beam parameters,
* study the effect of web and flange tapering on distortional buckling of I-beams,
* study the effect of various braces (i.e. the lateral brace, the rotational brace, the full brace) and their location on bucking load of cantilevers,
* to demonstrate the significance of incorporating distortional buckling as against studying lateral buckling only by treating the section as rigid.

CHAPTER II

PROBLEM FORMULATION

2.1 General

In this chapter, the finite element formulation is presented for analyzing the distortional buckling of mono-symmetric cantilever I-beams. The method is similar to that described by Bradford and Trahair (1981) and by Bradford (1991) for prismatic members having doubly symmetric sections. But, in using uniform elements to model a tapering mono-symmetric beam, one may expect a slow rate of convergence. It is, therefore, desirable to develop a tapered finite element that accurately represents a tapered member and does not introduce any artificial discontinuities at node points. The method requires a lengthwise subdivision of beam into one dimensional elements, for which the stiffness equations for buckling are developed.

The axis system of each element is shown in Fig. 2.1(a). The z-axis is the longitudinal axis, while the x- and the y-axes are the major and the minor principal axes, respectively. The actions of various loads on the beam element are shown in Fig 2.1(b), and are applied initially in the plane of symmetry y-z. The initial action set is W1, M1 and V1 at the end 1 (i.e. z=0) and W2, M2 and V2 at the end 2 (i.e. z=L); these actions are increased proportionally by the load factor λ until buckling occurs.

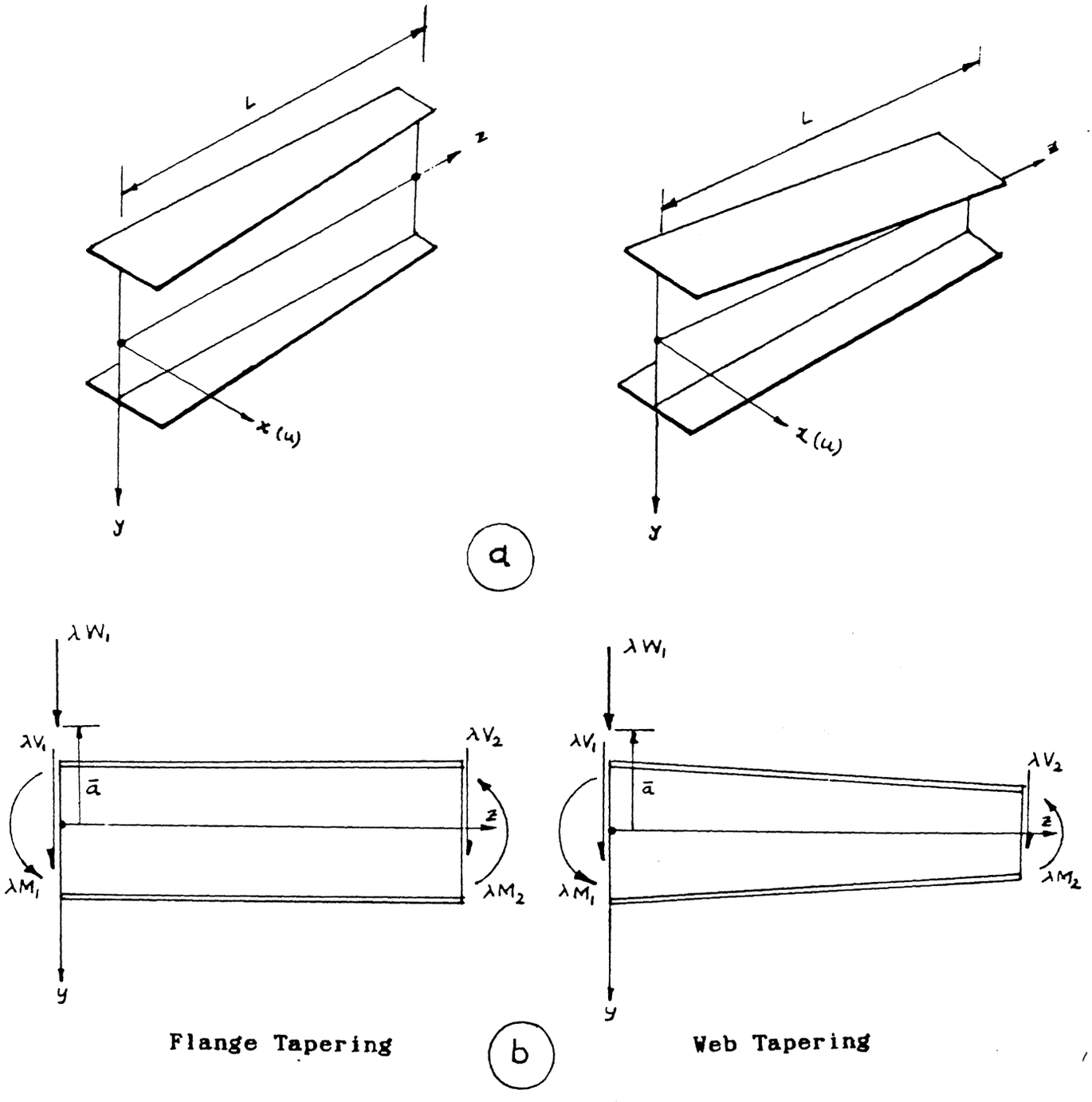

Fig. 2.1 ELEMENT AXIS IN Y-Z PLANES

(a) Beam-Column Element ,(b) Element Action In Y-Z Plane

2.2 Section Properties

Following parameters are found convenient to define the section properties :

(i) Mono-symmetry parameter (ρ)

$$\rho = \frac{I_{yt}}{I_{yt} + I_{yb}} \tag{2.1}$$

where I_{yt} and I_{yb} are the moments of inertia about the y-axis of the top and the bottom flanges, respectively. The parameter ρ=1 represents a T-section, ρ = 0.5 represents a doubly symmetric I-section, whereas ρ=0 corresponds to an inverted T-section.

(ii) Polar moment of inertia (J)

for thin open cross-sections it can be approximated as

$$J = \frac{1}{3} \sum_{i=1}^{n} b_i \, t_i^3 \tag{2.2}$$

where b_i and t_i are the length and the thickness of i^{th} member, respectively.

(iii) Beam parameter (k)

$$\bar{k} = \sqrt{\frac{\Pi^2 \, E \, I_y h^2}{4 \, G \, J \, l^2}} \tag{2.3}$$

where I_y is the moment of inertia of the whole section about the y-axis and l is the length of the beam. E and G are the modulus of elasticity and the modulus of rigidity, respectively.

2.3 Longitudinal Variation of Displacement

The cross-section of the beam is assumed to consist of two rigid flanges connected by a flexible web which may distort in the plane of the cross-section. The displacement of a cross-section of a beam element is shown in Fig.2.2 . When the beam buckles, its flanges deflect u_t and u_b, rotate u_t and u_b , and twist ϕ_t and ϕ_b, where a prime ( )′ indicates differentiation with respect to z. The lateral displacements of the flanges are assumed to be cubic polynomials, so that

$$\begin{aligned} u_t &= \alpha_1 L + \alpha_2 L Z + \alpha_3 L Z^2 + \alpha_4 L Z^3 \\ u_b &= \alpha_5 L + \alpha_6 L Z + \alpha_7 L Z^2 + \alpha_8 L Z^3 \end{aligned} \tag{2.4}$$

where Z = z/ L, and L being the length of elements. The flange twist may be expressed as

$$\begin{aligned} \Phi_t &= \frac{u_t - u_b}{h} + \alpha_9 + \alpha_{10} Z \\ \Phi_b &= \frac{u_t - u_b}{h} + \alpha_{11} + \alpha_{12} Z \end{aligned} \tag{2.5}$$

in which h is height of the section. Eqs. (2.4) and (2.5) may be expressed in matrix form by

$$\{ u \} = [M] . \{ \alpha \} \tag{2.6}$$

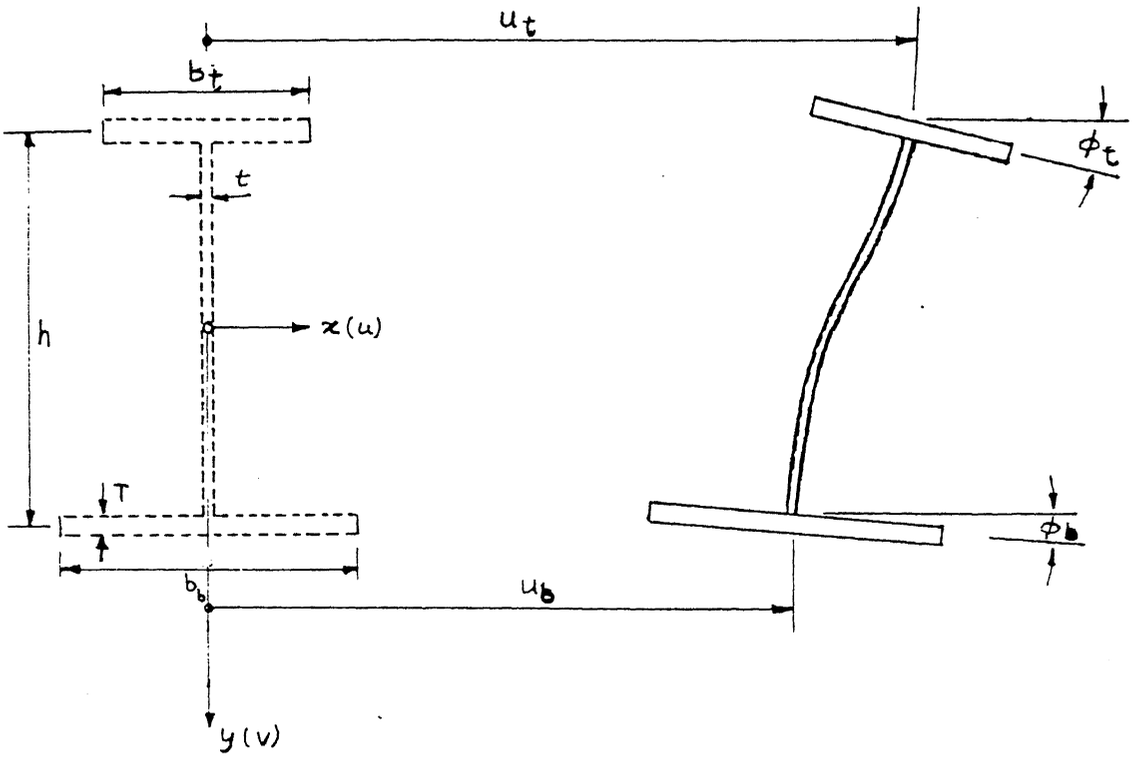

(a) Deformation In The Plane Of Cross-section

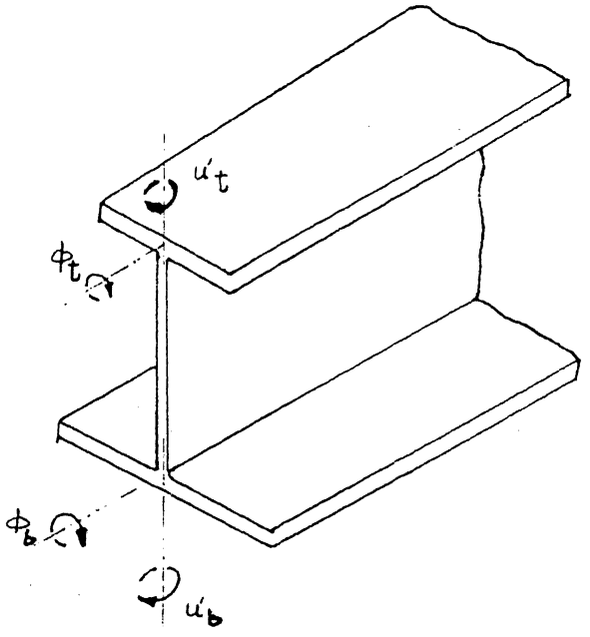

(b) Flange Rotations

Fig. 2.2 ELEMENT DISPLACEMENTS

in which

$$\{ u \} = \{ u_t, u_b, \varphi_t, \varphi_b \}^T$$
$$\{ \alpha \} = \{ \alpha_1, \alpha_2, \alpha_3, \ldots\ldots, \alpha_{10}, \alpha_{11}, \alpha_{12} \}^T \quad (2.7)$$

and [M] is given in Appendix -I. The nodal displacement vector $\{ \delta \}$ can be represented as

$$\{ \delta \} = \left\{ u_{t1}, u_{t2}, u'_{t1}, u'_{t2}, u_{b1}, u_{b2}, u'_{b1}, u'_{b2}, \varphi_{t1}, \varphi_{t2}, \varphi_{b1}, \varphi_{b2} \right\}^T \quad (2.8)$$

which represents the degree of freedom of nodes 1 and 2 of the element. By using eq. (2.7) the vector $\{ \delta \}$ can be expressed as

$$\{ \delta \} = [C] \{ \alpha \} \quad (2.9)$$

and so

$$\{ \alpha \} = [C]^{-1} \{ \delta \} \quad (2.10)$$

The matrix $[C]^{-1}$ is given in Appendix -II.

2.4 Cross-sectional Variation of Displacements

Since the flanges are assumed to be rigid, the vertical displacement of any flange point x is either

$$v_t = x \, \phi_t \quad \text{or} \quad v_b = x \, \phi_b \quad (2.11)$$

Moreover, it is assumed that the web becomes a cubic curve; thus the deflection at any point y can be written as

$$u_w = \{ \alpha_{13} + \alpha_{14} Y + \alpha_{15} Y^2 + \alpha_{16} Y^3 \} \; f(z) \qquad (2.12)$$

in which $Y = 2y/h$ and f is a cubic function of z . Using the identities

$$u_t = (u_w)_{-h/2} \qquad \phi_t = -\left(\frac{\partial u_w}{\partial y} \right)_{-h/2}$$

$$u_b = (u_w)_{h/2} \qquad \phi_b = -\left(\frac{\partial u_w}{\partial y} \right)_{h/2} \qquad (2.13)$$

the web displacement u_w can be expressed in terms of the vector of nodal displacement $\{ \delta \}$ by

$$u_w = \{ N \} \; [C]^{-1} \; \{ \delta \} \qquad (2.14)$$

The vector

$$\{ N \} = \{ N_w \} \; [C_w]^{-1} \; [M] \qquad (2.15)$$

is given in Appendix -III

2.5 Element Stiffness Matrix

During buckling, the beam element deflects and twists. The increase U in the strain energy during buckling can be approximated by

$$U = U_{fu} + U_{f\varphi} + U_w \qquad (2.16)$$

in which

U_{fu} = the flange in-plane bending strain energy.

$$= \frac{1}{2} \int_0^L EI_{yft} \left(u_t'' \right)^2 + EI_{yfb} \left(u_b'' \right)^2 dz \qquad (2.17)$$

where I_{yft} and I_{yfb} are the moments of inertia about the y-axis of top and bottom flanges, respectively.

$U_{f\phi}$ = the flange out of plane bending and twisting energy

$$= \frac{1}{2} D_f \int_0^L \left[\int_{-b_t/2}^{b_t/2} \left(V_t'' \right)^2 + 2 (1 - \nu) \left(\frac{\partial^2 V_t}{\partial x \, \partial z} \right)^2 dx \right]$$

$$+ \left[\int_{-b_b/2}^{b_b/2} \left(V_b'' \right)^2 + 2 (1 - \nu) \left(\frac{\partial^2 V_b}{\partial x \, \partial z} \right)^2 dx \right] \quad (2.18)$$

where ν is the Poisson's ratio and $D_f = E T^3 / 12 (1-\nu^2)$ and b_t and b_b are the width of top and bottom flanges, respectively.

UW = the strain energy of web

$$= \frac{1}{2} \int_0^L \int_{-h/2}^{h/2} \{ \varepsilon \}^T \{ \sigma \} \, dy \, dz \quad (2.19)$$

In eq. (2.19), the web generalized strain vector $\{ \varepsilon \}$ is

$$\{ \varepsilon \} = \left\{ \frac{\partial^2 u_w}{\partial^2 y} , \frac{\partial^2 u_w}{\partial^2 z}, - 2 \frac{\partial^2 u_w}{\partial y \, \partial z} \right\} \quad (2.20)$$

while the generalised stress vector is given by

$$\{ \sigma \} = [D_w] \{ \varepsilon \} \quad (2.21)$$

in which

$$[\ D_w\ ] = \frac{E\ T^3}{12\ (1-\upsilon^2)} \begin{bmatrix} 1 & \upsilon & 0 \\ \upsilon & 1 & 0 \\ 0 & 0 & \frac{(1-\upsilon)}{2} \end{bmatrix} \tag{2.22}$$

The stiffness matrix [k] of a beam element can be derived by expressing the strain energy in the form

$$U = \frac{1}{2}\ \{\ \delta\ \}^T\ [\ k\ ]\ \{\ \delta\ \} \tag{2.23}$$

Substituting eqs.(2.17) into eq. (2.16) and noting that eq. (2.16) and eq. (2.23) apply for all { δ }, lead to stiffness matrix

$$[\ k\ ] = [\ C\ ]^{-T}\ [\ k_\alpha\ ]\ [\ C\ ]^{-1} \tag{2.24}$$

The procedure of calculating the elements of stiffness matrix [k_α] is explained through an example in Appendix -IV.

2.6 Element Stability Matrix

The beam is subjected to bending moment and shear forces. The decrease in the potential energy of these actions during buckling is given by

$$V = V_{fu} + V_{f\phi} + V_w \tag{2.25}$$

in which

V_{fu} = the work associated with the in-plane flange deformation

$$= \frac{1}{2} \int_0^L \left[\ A_{ft}\ \sigma_t\ \{\ u_t'\ \}^2 + A_{fb}\ \sigma_b\ \{\ u_b'\ \}^2\ \right] dz \tag{2.26}$$

where A_{ft}, A_{fb} are the areas of and σ_t, σ_b are the bending stresses in the top and the bottom flanges, respectively,

$V_{f\phi}$ = the work done associated with the out-of plane flange deformations

$$= \frac{1}{2} T \int_0^L \left[\int_{-b_t/2}^{b_t/2} \sigma_t \{ v_t' \}^2 + \int_{-b_b/2}^{b_b/2} \sigma_b \{ v_b' \}^2 dx \right] dz \qquad (2.27)$$

V_w = the work associated with the web deformations

$$= \frac{1}{2} t \int_0^L \int_{-h/2}^{h/2} \begin{Bmatrix} \frac{\partial u_w}{\partial z} \\ \frac{\partial u_w}{\partial y} \end{Bmatrix}^T \begin{bmatrix} \sigma & \tau \\ \tau & 0 \end{bmatrix} \begin{Bmatrix} \frac{\partial u_w}{\partial z} \\ \frac{\partial u_w}{\partial y} \end{Bmatrix} dy\, dz \qquad (2.28)$$

where $\sigma = \lambda \frac{M_x}{I_x} y, \quad \tau = \lambda \frac{V}{h.t}$ (2.29)

In eq.(2.29) M_x is the moment about x-axis, V is the shear force at that section and I_x is the moment of inertia about the x-axis.

The element stability matrix $\lambda [g]$ is obtained from the decrease in potential energy V by a procedure analogous to the one described for the stiffness matrix in the section 2.6, and is given by

$$\lambda [g] = \lambda [C]^{-T} [g_a] [C]^{-1} \qquad (2.30)$$

2.7 The Work Done by Loads not at Shear Centre

It is well known that when a concentrated load W acts

at a height $\bar{a}$ above the shear center of the beam, the lateral buckling resistance is lowered because of the additional torque $W.\bar{a}.\phi$ which increases twisting of the beam. When the load λW_1 at element node 1 acts within the web height $\bar{a}$ above the shear center the point is lowered by $\frac{1}{2}\int_0^{\bar{a}} (\partial u_w / \partial y)^2$; hence the loss of potential energy is given by

$$Vd = \frac{\lambda w_1}{2} \int_0^{\bar{a}} \left(\frac{\partial u_w}{\partial y} \right)^2 dy \quad , \qquad -h/2 \leqslant \bar{a} \leqslant h/2 \qquad (2.31)$$

The inclusion of the load height in finite element model was achieved by calculating and adding separately these terms to stability matrix $\lambda [g]$.

2.8 Effect of Mono-symmetry

When a beam of mono-symmetric section is loaded in its plane of symmetry, it twists during buckling and the longitudinal bending stress $M_x y / I_x$ exerts torque. The action of this torque is to change the effective rigidity of the beam. The compressive bending stress causes a disturbing torque while the tensile stress a gives a restoring torque. In a doubly symmetric section, these two torques balance each other. On the other hand, in a mono-symmetric section there is an imbalance torque which depends upon the lever arm between the flanges and the shear center. Since in the present investigation the web distortion is being taken into consideration, the location of the shear centre is a difficult proposition. Hence, for calculating the work done by the imbalance torque, it is assumed that the shear center lies on the straight line joining the top and the bottom flanges. Accordingly , this work done can be expressed as

$$V = \frac{1}{2} \int_0^L \lambda M_x \beta_x (\phi_{avg})^2 \, dy \qquad (2.32)$$

in which $$\beta_x = \frac{1}{I_x} \int_A (x y^2 + y^3) \, dA + 2 \bar{y} \quad ,$$

$$\phi_{(avg.)} = (u_t - u_b) / h \quad ,$$

and $\bar{y}$ is the depth of shear center from the top flange.

2.10 Global Stiffness and Stability Matrices

The global stiffness matrix [K] and stability matrix [G] can be assembled from the individual element stiffness and stability matrices [k] and [g], respectively, using equilibrium and compatibility at nodes. The numerical integration with respect to x,y and z is carried out using the four-point Guassian-quadrature. The total potential Π may be written as

$$\Pi = \frac{1}{2} \{ Q \}^T \left([K] - \lambda [G] \right) \{ Q \} \qquad (2.33)$$

where { Q } is the vector of global degrees of freedom assembled from the { q } vectors of each element. Invoking the principle of stationary potential energy yields

$$\delta\Pi = \{ \delta Q \}^T \left([K] - \lambda [G] \right) \{Q\} = 0 \qquad (2.34)$$

Noting that the variations { δQ } are arbitrary, this results in

$$\left([K] - \lambda [G] \right) \{ Q \} = 0 \qquad (2.35)$$

The values of λ which yield a non trivial solutions for $\{ Q \}$ in eq. (2.35) are the eigen-values, while the corresponding values of $\{ Q \}$ are the eigen-vectors. For a non-trivial solution

$$\left| [K] - \lambda [G] \right| = 0 \qquad (2.36)$$

The above eigen-value equation is solved using the 'NAG-LIBRARY' subroutine 'F02BJFE.f'. The critical load is given by lowest positive eigen-value.

CHAPTER III

RESULTS AND DISCUSSION

3.1 Introduction

The finite element formulation developed in chapter II is used to study the lateral/distortional buckling of mono-symmetric, tapered, braced cantilever I-beams, under a concentrated point load at the free end. As mentioned earlier, the main assumption in the formulation has been that the flange remains undistorted during buckling. Because of this assumption the local buckling for low h/t ratio (web height to thickness ratio) can not be predicted accurately (Hancock, 1978,1980).

Since tabulated closed-form solution for distortional buckling are not available for mono-symmetric, tapering or braced cantilevers, the stiffness and the stability matrices generated are tested by comparing value of buckling load with available results (Bradford, 1988; Trahair, 1986) for beams with rigid web. To reduce the distortional buckling case to the rigid web case (i.e. lateral torsional buckling) the plate rigidity, D_w , for the out-of-flange flexure of web is made to approach infinity.

The geometric parameters of the beam cross-section are shown in Fig. 2.1. In presenting the results of the effect of mono-symmetry on the distortional buckling, the distortional load, W_{od}, is normalized with respect to the lateral buckling load, W_{or},(i.e. considering the

web as rigid). On the other hand, in discussing the effect of flange and web tapering on distortional buckling, the load is non-dimensionalised $W l^2/\sqrt{(EI\ GJ)_o}$ in terms of beam parameters. Throughout, the value of Young's modulus is taken as 2×10^8 kN/ m^2 and that of Poisson's ratio as 0.3.

3.2 Accuracy and Convergence

The distortional buckling of cantilever beams with concentrated load at the shear centre of the free end was considered by Johnson and Will (1974). The geometrical parameters were : h = 533 mm., $b_b = b_t = 254$ mm, l = 3810 mm. In their analysis, two relatively fine meshes of rectangular elements were used. One mesh consisted of 60 elements (20 in the web, 20 in each flange), while the second consisted of 96 elements (48 in the web and 24 in each flange). The buckling loads for the two cases were 1410 kN and 1370 kN, respectively. Using the present formulation, the buckling loads are 1413 kN ,1405 kN and 1403 kN for 4,8 and 10 longitudinal elements, respectively. The lowest value (1403 kN) differs by 2.4 % from that of Johnson and Will (1974). The rate of convergence of the finite element method is investigated for a doubly-symmetric beam, both with tapered web ($\beta = 0.5$) and with tapered flange($\alpha = 0.5$), with point load applied at the shear centre and at the top flange.

Fig 3.1 shows the convergence of the non-dimensional load, $W l^2/\sqrt{(EIGJ)_o}$, with the number of elements (the subscript o refers to

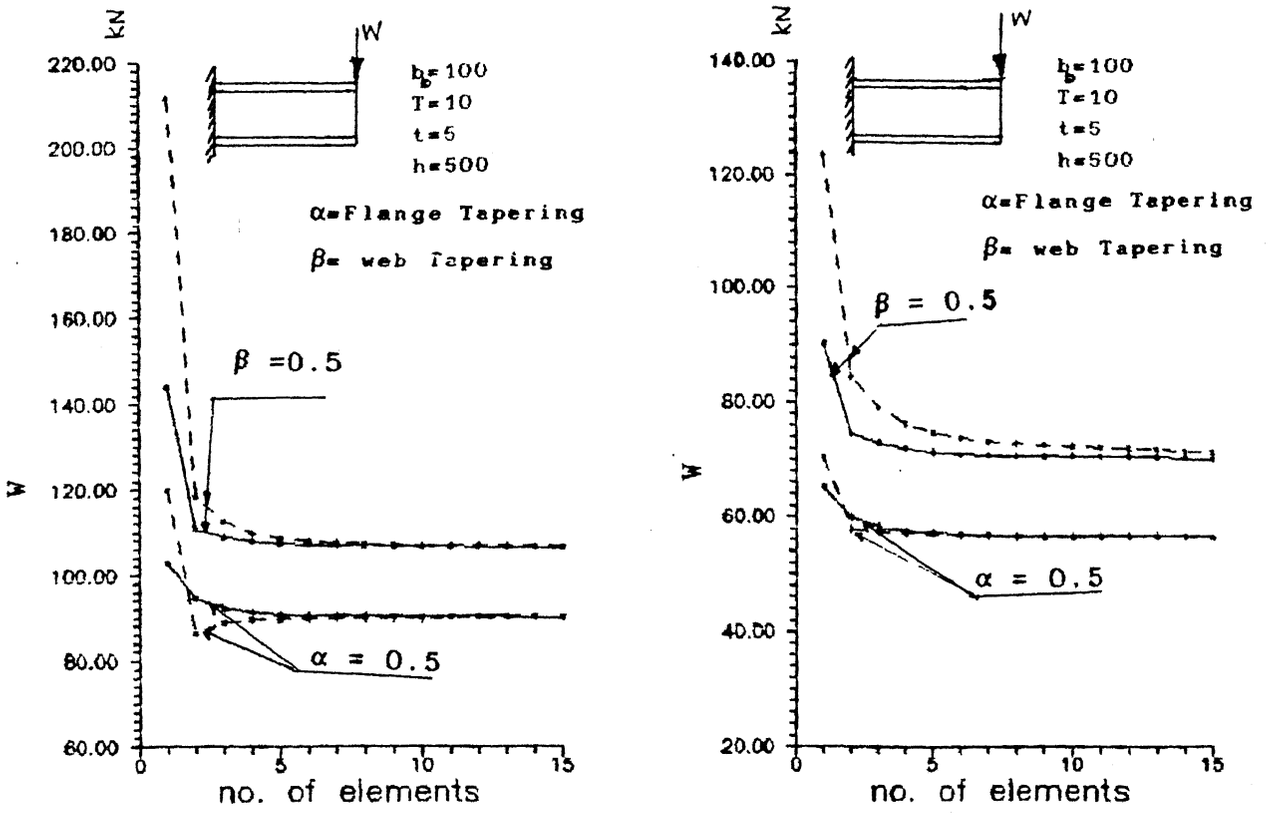

Fig. 3.1 CONVERGENCE OF BUCKLING LOAD FOR CANTILEVER

(———) Tapered Element , (-----) Stepped Element

the values at the fixed end). It can be seen that the convergence is very rapid in case of tapered element; the load remains more or less constant for four or more elements. Moreover, the convergence is faster while considering the effect of the flange taper than that of the web taper. It is also observed that the top flange loading requires comparatively more number of elements as compared to the shear centre loading. In any case, minimum of ten elements are used to model the beam.

3.3 Effect of Mono-symmetry

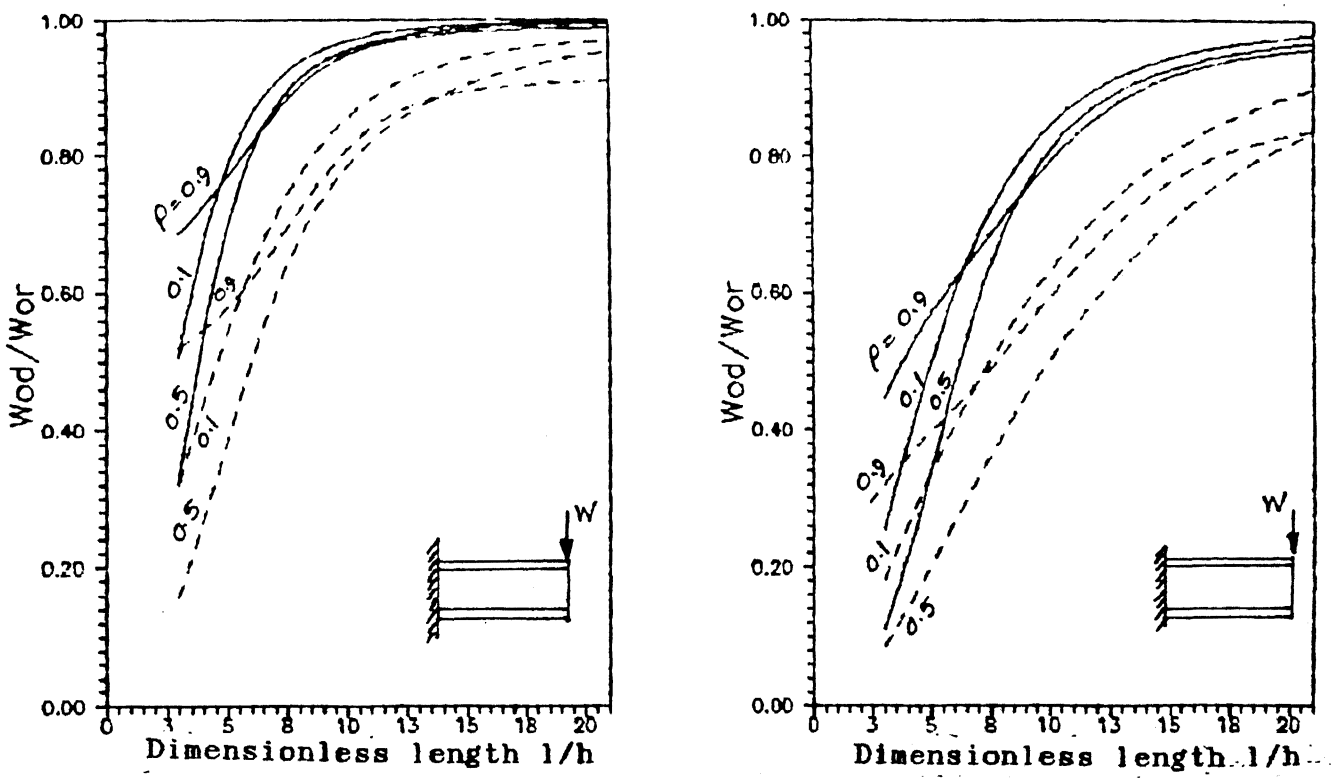

$b_b/T = 10$ $b_b/h = 0.2$ $b_b/T = 15$ $b_b/h = 0.4$

Fig 3.2 EFFECT OF MONO-SYMMETRY ON DISTORTIONAL BUCKLING.
(Shear Centre Loading)

(———) h/t=100 (----) h/t=250

Figures. 3.2 and 3.3 show the effect of mono-symmetry on the distortional buckling of I-beams. Similar to the case of lateral-torsional buckling, the beam having the bigger flange in compression gives higher buckling load than the beam with equal flanges or with smaller flange in compression, for the same value of the beam parameter $\bar{K}$. To demonstrate how the distortion affects the buckling load when flanges are unequal, the distortional buckling load , W_{od}, is

normalized with respect to lateral-torsional buckling load, W_{or}, and the results are plotted against l/h ratio for different values of the mono-symmetry parameter ρ. Since the compression flange width to the height ratio (b_b/ h) is also one of the influencing parameter, the tension flange width b_t varied (keeping the compression flange width b_b constant) in order to get various values of ρ.

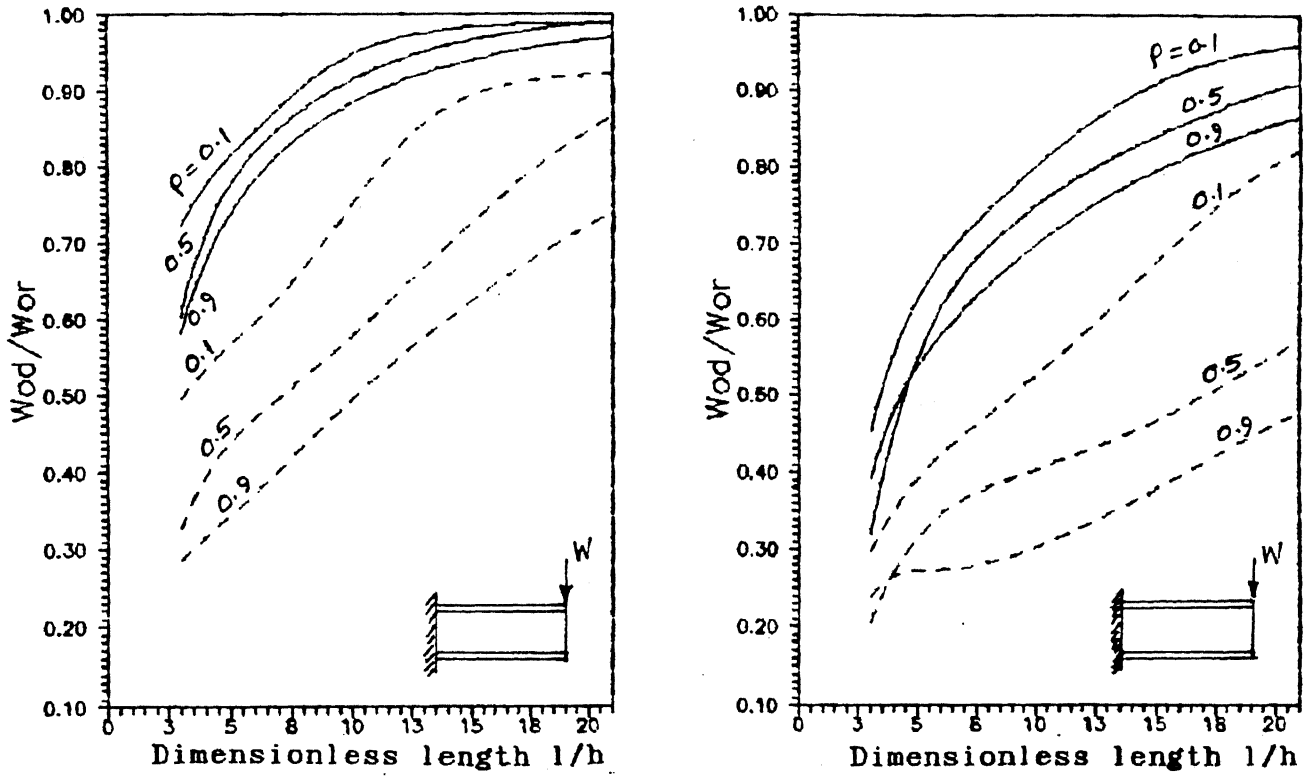

$b_b/T = 10$ $b_b/h = 0.2$ $b_b/T = 15$ $b_b/h = 0.4$

Fig 3.3 EFFECT OF MONO-SYMMETRY ON DISTORTIONAL BUCKLING.

(Top Flange Loading)

(———) h/t=100 (----) h/t=250

Figures 3.2 and 3.3 show that as the degree of mono-symmetry decreases, the reduction in the buckling load ratio also decreases, i.e. bigger the compression flange lesser is the distortional buckling load. Further, as the b_b/h ratio increases, the effect of distortion on buckling load becomes prominent. It can also be observed that the effect of web distortion becomes pronounced with the increase in the h/t ratio i.e. when the web becomes more slender. Moreover, as the l/h ratio decreases, the distortional buckling load gets reduced significantly.

For the top flange loading, although the nature of the curves are similar (Fig. 3.3) the effect of mono-symmetry is more than that in the shear centre loading. Also, the trend in the result as the degree of mono-symmetry varies from ρ = 0.1 to 0.9 is quite different than what is observed when load is at the shear centre.

3.4 Effect of Flange / Web Tapering

Two cases of tapering are considered : (i) flange tapering, measured in term of parameter α (ratio of the flange width at the free end to that at the fixed end), (ii) web tapering, measured in term of parameter β (ratio of the web height at the free end to that of at the fixed end). Fig. 3.4-3.7 illustrate the effect of web and the flange tapering on distortional buckling for the shear centre loading and the top flange loading. The non-dimensionalised buckling load $W l^2/\sqrt{(EIGJ)_o}$, is plotted against the beam parameter $\bar{K}\left(=\Pi\sqrt{(EI_y h^2/4GJL^2)_o}\right)$. For the sake of comparison, the corresponding

results for lateral buckling are also given in all figures.

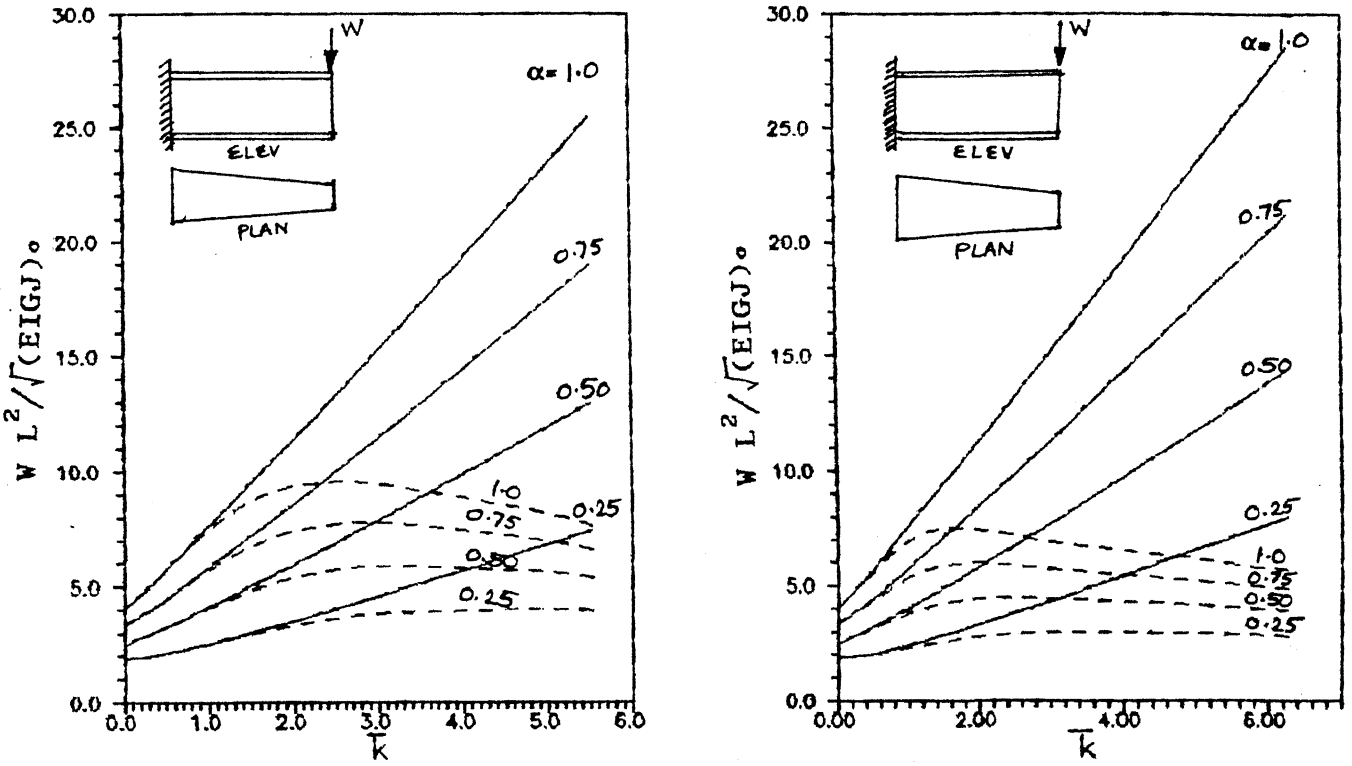

h/t=100 h/t=250

Fig. 3.4 EFFECT OF FLANGE TAPERING ON DISTORTIONAL BUCKLING

(Shear Centre Loading)

(———) Lateral-Torsional Buckling, (----) Distortional buckling

Fig. 3.4 shows the the effect of the flange tapering on the distortional buckling load for the shear centre loading. As the flange tapering increases (α changes from 1.0 to 0.25) the net decrease in the load also goes down i.e more the flange tapering, less will be the distortional effect. The h/t ratio also affects the distortional buckling capacity for given values of flange tapering (α) of beams; the loss in strength is more for higher h/t ratios.

Similarly Fig. 3.5 shows the effect of web tapering. For $\bar{K}$ lying in the range 1.0-4.0, there is a significant difference in the loss of strength due to distortion, but for $\bar{K}$ > 4.0 the loss in strength for each value of the web tapering parameter β is approximately the same. Further, the increase in the h/t ratio decreases the net buckling load capacity.

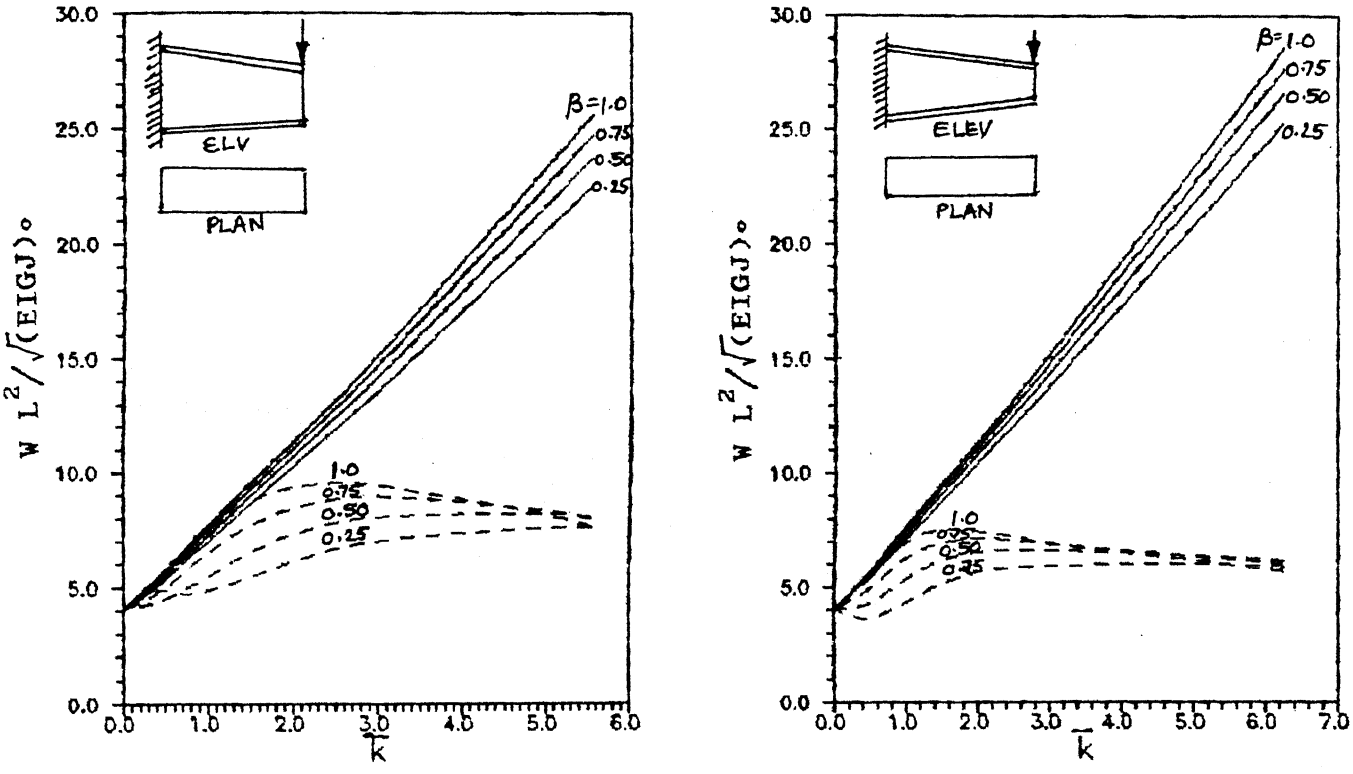

Fig. 3.5 EFFECT OF WEB TAPERING ON DISTORTIONAL BUCKLING

(Shear Centre Loading)

(———) Lateral-Torsional Buckling, (----) Distortional buckling

From Figures 3.6 it can be seen that for the top flange

loading, the loss of strength due to distortion is approximately the same for all values of α (flange tapering),when the load is at the top flange. Moreover, the loss of strength due to distortion is more in a slender web (high h/t ratio) than in a stocky web.

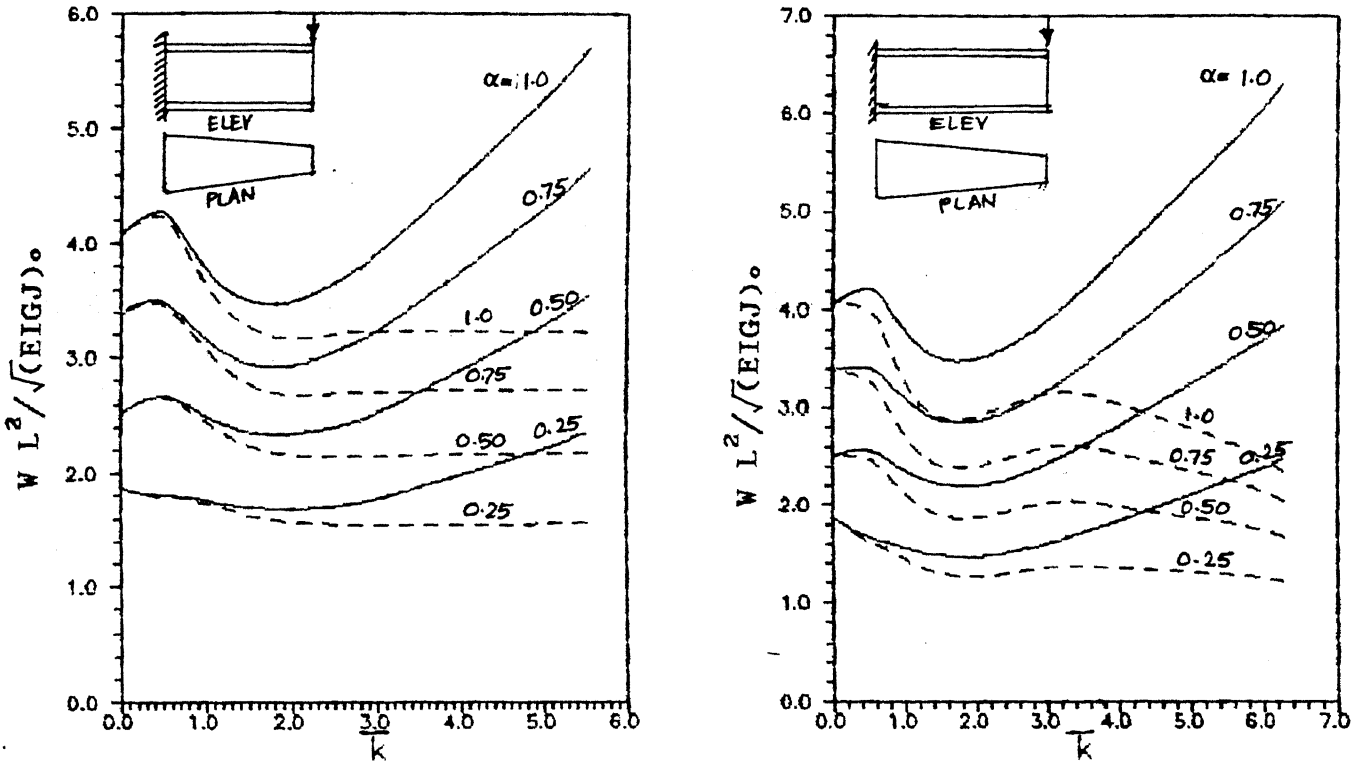

Fig. 3.6 EFFECT OF FLANGE TAPERING ON DISTORTIONAL BUCKLING
(Top Flange Loading)
(———) Lateral-Torsional Buckling, (----) Distortional buckling

The effect of web tapering on the buckling of cantilevers when the point load is at the top flange can be seen in Fig. 3.7. Both the values of h/t, 100 and 250, are considered. The effect of distortion increases as the web tapering increases (i.e. β decreases). The effect is more pronounced for higher h/t ratios (slender webs).

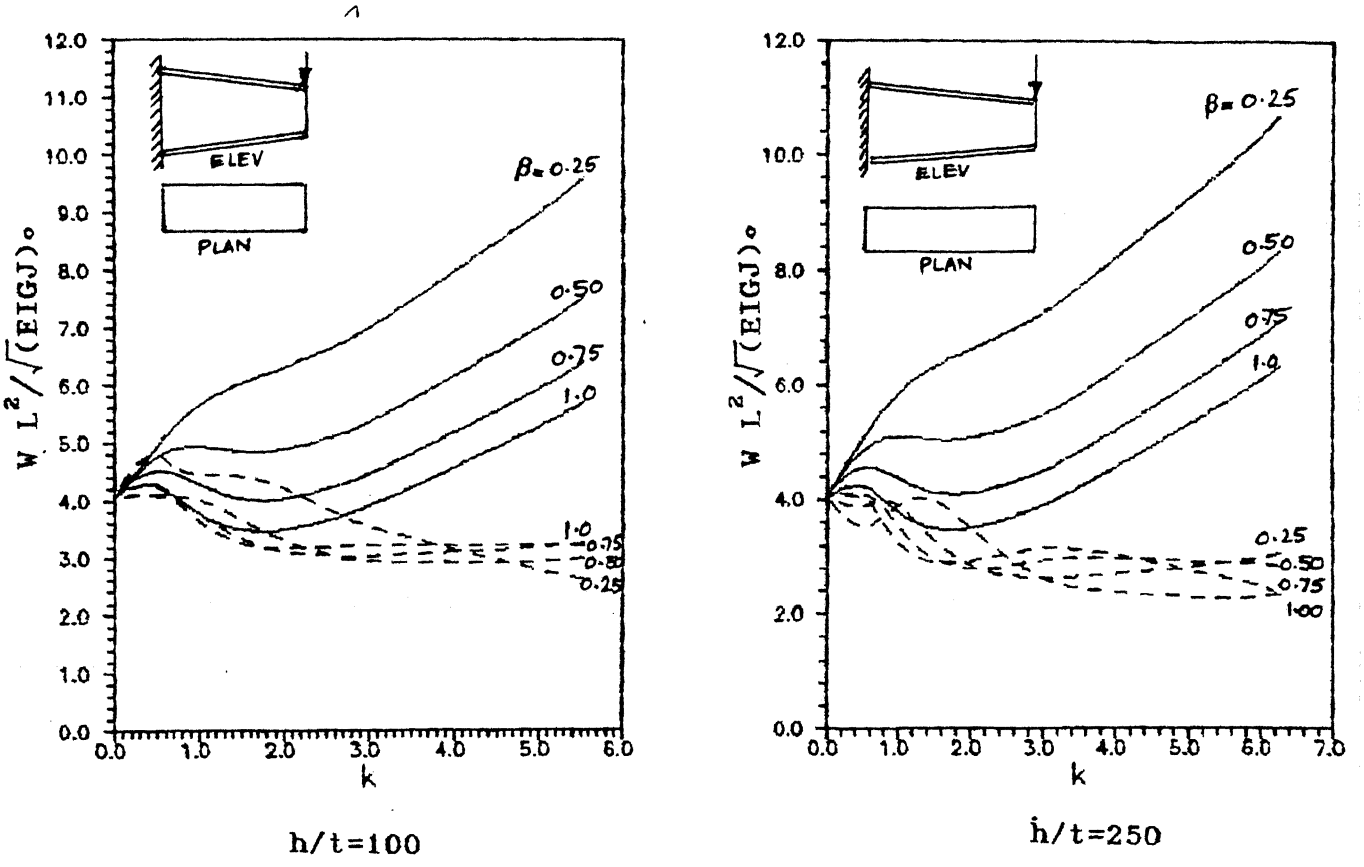

Fig. 3.7 EFFECT OF WEB TAPERING ON DISTORTIONAL BUCKLING

(Top Flange Loading)

(———) Lateral-Torsional Buckling, (----) Distortional buckling

3.5 Braced Cantilevers

The elastic buckling capacity of mono-symmetric cantilevers with braces is influenced by following factors : (i) type of brace- i.e full brace(fb), lateral brace at the top flange (lt) , lateral brace at the bottom flange(lb), rotational brace at the top flange(rt), rotational brace at the bottom flange (rb), (ii) location of brace, (iii) degree of mono-symmetry (v) web slenderness ratio. Due to large number of influencing parameters, it is difficult to present results comprehensively covering all the ranges. However, an attempt is made to

examine their effect separately.

The effect of a particular brace depends upon how stiff the brace is. Normally braces having stiffness two or three times the beam stiffness in that direction are sufficient to reduce the displacement at that point nearly to zero. In this investigation, the brace stiffness are assumed to be infinite, which means that the corresponding displacement at that point is completely restrained. Five values of mono-symmetry parameter ρ are taken for investigating the brace effect with the point load at the shear centre and at the top flange.

First, a symmetric I-section with two web slenderness ratios is considered to demonstrate the effect of each brace. The full brace appears to be more effective for all portions of the beam compared to other braces as it prevents all the degrees of displacement at the point. The lateral brace at the top flange is more effective than at the bottom flange. While the optimum location for the top flange lateral brace is near the free end, it is somewhere near the mid-span for the bottom flange lateral brace. Rotational braces are less effective than lateral braces. The top flange rotational brace is more effective than bottom flange rotational brace near mid-span of the beam while the situation is just the reverse near the free end. Further, as expected, the effectiveness of braces increases with the decrease in web slenderness ratio, i.e. efficiency is more in stocky webs than slender webs.

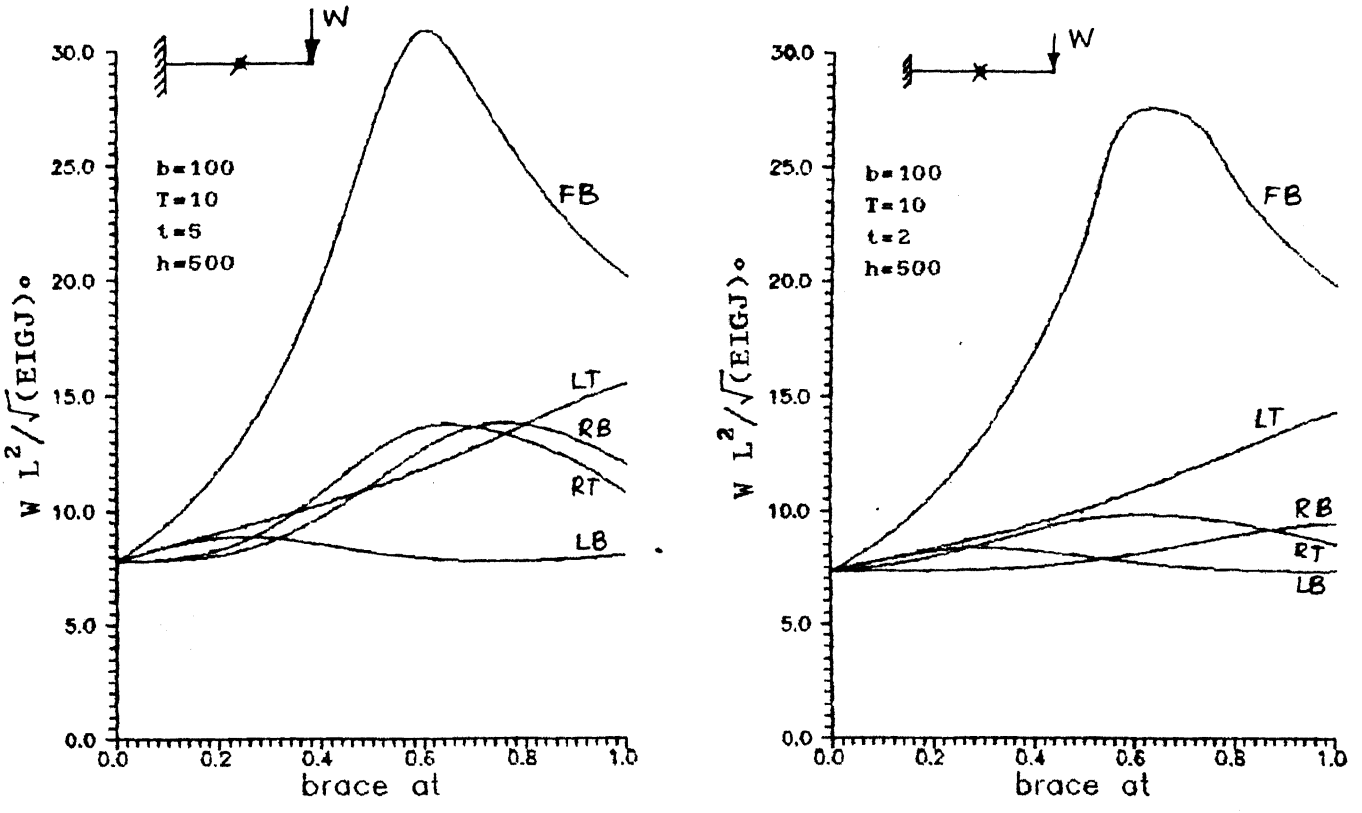

Fig 3.8 EFFECT OF BRACE LOCATION ON BUCKLING LOAD FOR DIFFERENT TYPES OF BRACES (Doubly Symmetric Section)

Figures 3.9 to 3.13 demonstrate the effect of the load position when different types of braces are considered for beams having varying degree of mono-symmetry. As expected, the buckling capacity increases as the load moves towards the shear centre.This is so because the distortional torque reduces as the load shifts from the top flange towards the shear centre.

As is evident from Fig. 3.8 to 3.13, in general the influence of a discrete brace is more beneficial in cantilever beams whenever the

compression flange is bigger than the tension flange. In contrast, for ρ = 0.9 the increase in the buckling capacity for nearly all types of braces (expect for lateral brace at the bottom flange for the top flange loading) is very small. For all degrees of mono-symmetry (ρ = 0.1 to 0.9) the optimum location of brace (for all types of brace) is approximately near the mid-span when the load is at the shear centre and it is near the free end for the top flange loading.

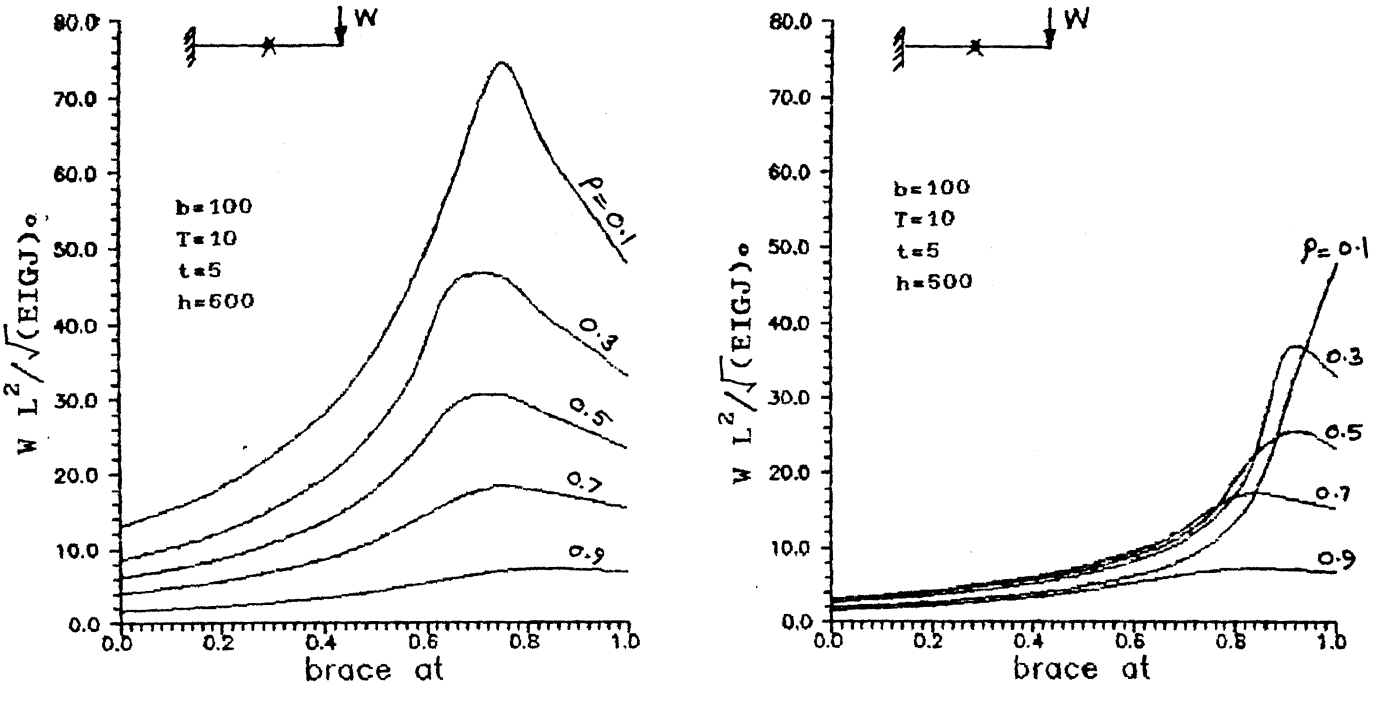

Shear Centre Loading

Top Flange Loading

Fig 3.8 EFFECT OF BRACE LOCATION ON BUCKLING LOADS (Full Brace)

For the shear centre loading, the lateral brace at the top flange is more effective than the bottom flange lateral brace and the optimum position of the brace is near the free end. For the top flange

loading, the bottom flange rotational brace is more effective than at the top flange. For the top flange rotational brace, the optimum location lies in the range 0.71 to 0.91, whereas for bottom flange rotational brace it is near the free end.

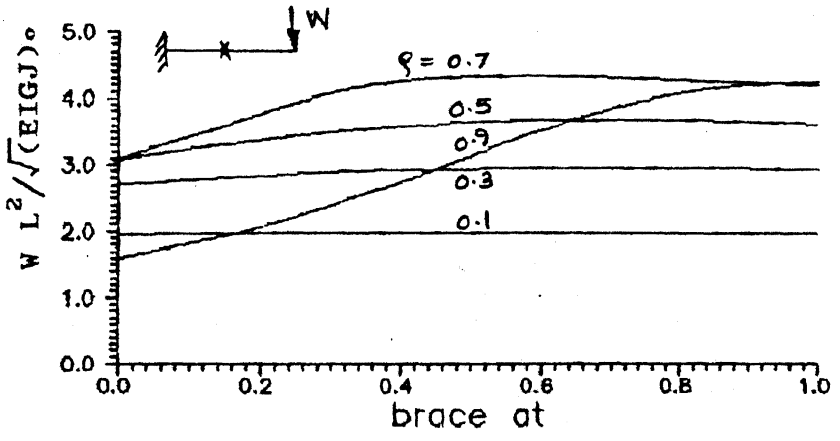

Top Flange Loading

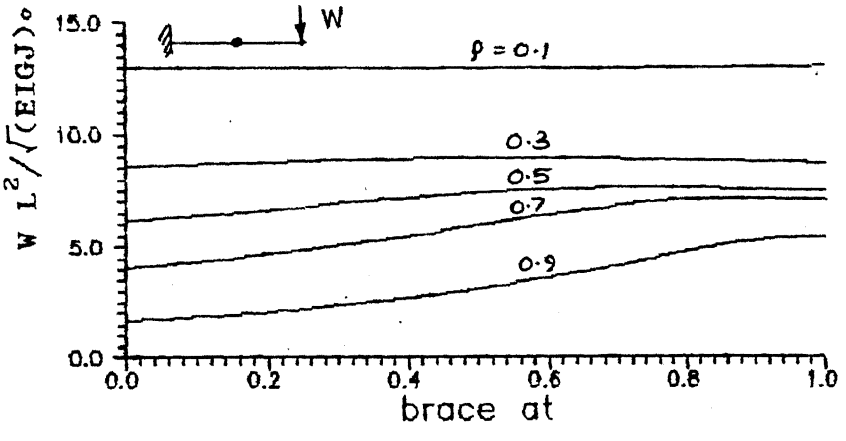

Shear Centre Loading

Fig 3.10 EFFECT OF BRACE LOCATION ON BUCKLING LOADS (Rotational Brace at the Bottom Flange)

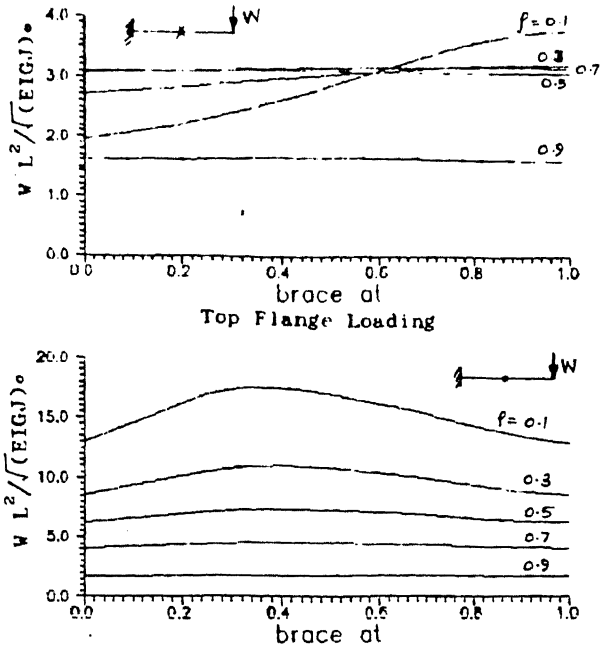

Fig 3.11 EFFECT OF BRACE LOCATION ON BUCKLING LOADS

(Rotational Brace at the top Flange)

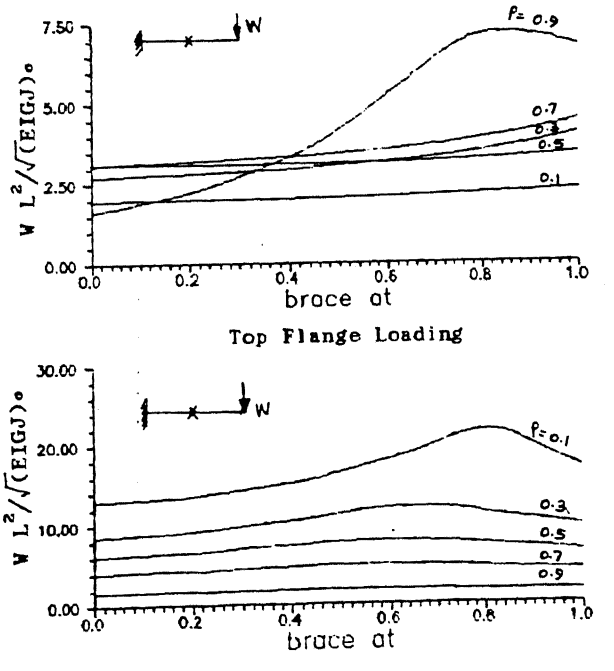

Fig 3.12 EFFECT OF BRACE LOCATION ON BUCKLING LOADS

(Lateral Brace at the Bottom Flange)

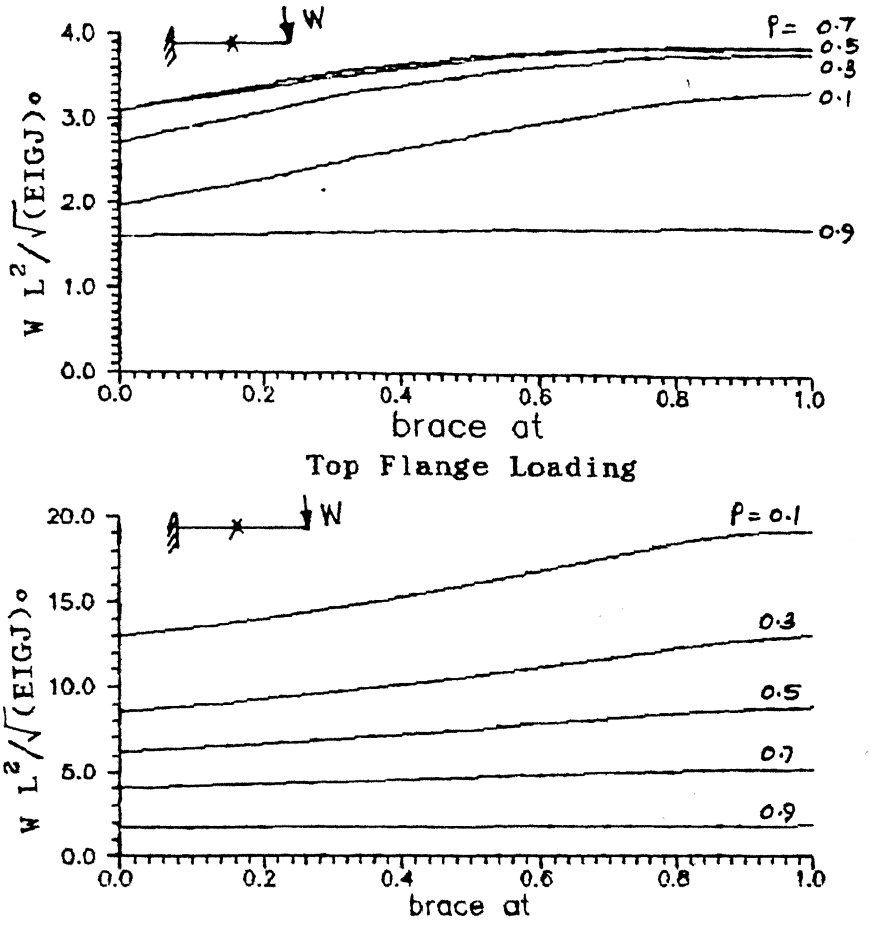

Fig 3.13 EFFECT OF BRACE LOCATION ON BUCKLING LOADS

(Lateral Brace at the Top Flange)

CHAPTER IV

CONCLUDING REMARKS

The finite element method of analysis has been presented which is capable of making fairly accurate determination of distortional buckling for tapered, mono-symmetric and braced cantilever I-beams. The accuracy of the method has been shown by comparison with some known results, and its rapid convergence has been demonstrated by comparing it with a finite-element representation that uses uniform elements. On basis of this study, some salient observations and results can be summarized as under:

- the reduction in the distortional buckling load is less for higher values of α, the flange tapering parameter.
- the reduction in the distortional buckling load is more for higher values of β, the web tapering parameter; it is definitely so for $\bar{k}$ up to 4.
- the effect of distortion on the lateral buckling load decreases with the increase in the size of compression flange.
- the loss of strength due to distortion is more in a beam with the top-flange loading than with the shear centre loading.
- in general the advantage of braces is more when the larger flange is under compression.
- although, the full brace is most effective; other braces are also reasonably effective when they restrain the top flange displacement.
- the optimum location of the brace is near the mid-span for the shear centre loading and near the free end for the top flange loading.

REFERENCES

- Anderson J. M. and Trahair N.S. (1972), " Stability Of mono-symmetric beams and cantilevers.", J. Struct. Engg., ASCE 98, ST1,pp. 267-278.

- Barosum R.S. and Gallaghar R.H. (1970), " Finite Element Analysis Of Torsional and Torsional-Flexure Stability Problems.", Int. J. Numeric. Methods Engg. 2, pp 335-352.

- Bradford M. A. and Trahair N. S. (1981), " Distortional Buckling Of I-Beams.", J. Struct. Div. ASCE 107 ,ST2, pp 355-370.

- Bradford M. A. (1988), " Buckling Of Elastically Restrained Beams With Web Distortions. ", Thin Walled Structures 6 , pp 287-304.

- Bradford M. A. (1990),. " Lateral-Distortional Buckling Of Tee-Section Beams.", Thin Walled Structures 10, pp 13-30.

- Bradford M. A. (1992), " Buckling Of Doubly Symmetric Cantilevers With Slender Web.", J. Engg. Struct, Vol 14, No 5, pp 327-334.

- Bradford M. A. and Geo Z. (1992), " Distortional Buckling Solution For Composite Beams.", J. Struct. Div ASCE 118(1), pp 73-89.

- Hancock G.J. (1978), " Local, Distortional And Lateral Buckling Of I-Beams.", J. Struct. Div. ASCE (100), ST11, Proc. Parer 14155, pp 2205-2222.

- Hancock G. J., Bradford M. A., and Trahair N. S. (1980), " Web Distortion And Flexure Torsional Buckling.", J. Struct. Div ASCE 106, ST 7, Proc. Paper 15593, pp 1557-1572.

- Johnson C. P. and Will K. M.(1974), "Beam Buckling By Finite Element Procedure", J. Struct. Div., Vol 100, ST 3, pp 669-685.

- Kitiporanchai S. and Trahair N. S. (1972), "Elastic Stability Of Tapered I-beams ", J. Struct. Div. ASCE 98, ST 3, pp 713-728.

- Kitiporanchai S. and Trahair N. S. (1975), " Elastic Behaviour Of Tapered Mono-symmetric I-Beams.", J. Struct. Div. ASCE (101), ST8, pp 1661-1678.

- Kitiporanchai S. and Trahair N. S. (1980), " Buckling Of Mono-symmetric Beams.", J. Struct. Div. ASCE (106), ST5, pp 941-957.

- Kitiporanchai S., Richter N. J. and Dux P. F. (1984), " Buckling And Bracing Of Cantilevers. ", J. Struct. Engrg ASCE 110, pp 2250-2262.

- Kitiporanchai S., Wang C. M. and Trahair N. S. (1986-a), "Buckling Of Mono-symmetric I-Beams Under Moment Gradient.", J. Struct. Engrg. ASCE 112(4), pp 781-799.

- Kitiporanchai S. and Wang C. M. (1990), " Integrated View Of Methods In Buckling Analysis.", Research report Series University of Queens-Land (Aus.), No. CE 117.

- Kumar A. and Shah N. H. (1991), " Lateral Buckling Of Mono-Symmetric I-beams", Int. J. Struct. 11(2), pp 119-130.

- Kumar A. and Shah N. H. (1993), " Lateral Buckling of Tapered Beam-Columns ", Int. J. Struct., 13(1) ,14-34.

- Robert T. M.and Jitta P.S.(1983), " Lateral, local And Distortion Buckling Of I-Beams.", Thin Walled Structures 1, pp 289-308.

- Taylor A. C. And Ojalvo M. (1965), "Torsional Requirement Of Lateral Buckling", J. Struct. Div. ASCE 19 , pp 115-129.

- Timoshenko S.P. and Gere J.M. (1961), " Theory Of Elastic Stability.", McGraw Hill New york.

▸ Trahair N.S. and Bradford M.A. (1988), " The Behaviour And Design Of Steel Structures." (second edition),Champman and Hall

▸ Wang C. M., Kitiporanchai S. and Thervendran V. (1986), " Buckling Of Braced Mono-symmetric Cantilevers.", Int. J. Mech. Sci. Vol 29, No. 5, pp 321-327.

▸ Wang C. M. and Kitiporanchai S. (1989), " New Set Of Parameter For Mono-symmetric Beam-Columns/ Tie-Beams.", J. Struct. Engrg ASCE 115(6), pp 1497-1513.

APPENDIX - I

Matrix [M] in Equation (2.7)

$$[M] = \begin{bmatrix} Mu & 0 & 0 & 0 \\ 0 & Mu & 0 & 0 \\ \frac{1}{h} Mu & \frac{-1}{h} Mu & M\Phi & 0 \\ \frac{1}{h} Mu & \frac{-1}{h} Mu & 0 & M\Phi \end{bmatrix}$$

$$\left\{ M_u \right\} = \left\{ L, \quad LZ, \quad LZ^2, \quad LZ^3 \right\}$$

$$\left\{ M_\Phi \right\} = \left\{ 1, \quad Z \right\}$$

and $\{ \alpha \} = \{ \alpha_1, \alpha_2, \ldots\ldots, \alpha_{12} \}^T$

APPENDIX - II

Matrix $[\ C\ ]^{-1}$ in Equation (2.10)

$$[\ C\ ]^{-1} = \begin{bmatrix} C_u & 0 & 0 \\ 0 & C_u & 0 \\ C_\phi \quad 0 & -C_\phi \quad 0 & -hC_\phi \quad 0 \\ C_\phi \quad 0 & -C_\phi \quad 0 & 0 \quad -hC_\phi \end{bmatrix}$$

in which

$$C_u = \begin{bmatrix} \frac{1}{L} & 0 & 0 & 0 \\ 0 & 0 & 1 & 0 \\ \frac{3}{L} & \frac{3}{L} & -2 & -1 \\ \frac{2}{L} & \frac{-2}{L} & 1 & 1 \end{bmatrix} \qquad C_\phi = \begin{bmatrix} \frac{1}{h} & 0 \\ 0 & \frac{1}{h} \end{bmatrix}$$

in which h is the distance between the centroid of the top and the bottom flanges, and L is the the length of an element.

APPENDIX - III

Vector { N } in Equation (2.14)

$$\{ N_w \} = \{ 1, Y, Y^2, Y^3 \}$$

$$[C_w]^{-1} = \frac{1}{8} \begin{bmatrix} 4 & 4 & -h & h \\ -6 & 6 & h & h \\ 0 & 0 & h & -h \\ 2 & -2 & h & -h \end{bmatrix}$$

$$\{ N \} = \frac{L}{8} \left\{ \begin{array}{c} 4 - 4Y \\ 4Z - 4YZ \\ 4Z^2 - 4YZ^2 \\ 4Z^3 - 4YZ^3 \\ 4 + 4Y \\ 4Z + 4YZ \\ 4Z^2 + 4YZ^2 \\ 4Z^3 + 4YZ^3 \\ -H + HY + HY^2 - HY^3 \\ -HZ + HYZ + HY^2Z - HY^3Z \\ H + HY - HY^2 - HY^3 \\ HZ + HYZ - HY^2Z - HY^3Z \end{array} \right\}$$

APPENDIX - IV

Procedure for Calculating Elements Of Stiffness Matrix

Using the eqs (2.6) and (2.10), we get

$$\{ u \} = [M] [C]^{-1} \{ \delta \}$$

and hence

$$D^n\{ u \} = D^n[M] [C]^{-1} \{ \delta \}$$

in which D^n is the differential operator of n^{th} order. Consider the first term on right hand side of eq. (2.17) which is strain energy stored due to lateral deformation of the top flange

$$U_{fut} = \frac{1}{2} \int_0^L E I_{yft} \{ u_t'' \}^2 dz$$

From eq (4.2) we can write

$$= \frac{1}{2} \int_0^L E I_{yft} \left[[M_t''] [C]^{-1} \{ \delta \} \right]^2 dz$$

$$= \frac{1}{2} \int_0^L \left[\{ \delta \}^T [C]^{-T} [M_t'']^T E I_{yft} [M_t''] [C]^{-1} \{ \delta \} \right] dz$$

$$= \{ \delta \}^T [C]^{-T} \frac{1}{2} \int_0^L [M_t'']^T E I_{yft} [M_t''] dz [C]^{-1} \{ \delta \}$$

where as $[M_t]$ is the corresponding shape function for $\{ u_t \}$.

We can now write

$$U_{fut} = \frac{1}{2} \{ \delta \}^T [k_{fut}] \{ \delta \}$$

in which

$$[k_{fut}] = [C]^{-T} [ka_{ut}] [C]^{-1}$$

$$[ka_{ut}] = \int_0^1 [M_t'']^T E I_{yft} [M_t''] \, dz$$

On similar lines we can evaluate second part of the right hand side of eq (2.17), and the right hand side of eqs. (2.18), (2.19) and combining them to get the element stiffness matrix $[k_a]$.